JOURNAL OF LAND USE SCIENCE, 2017
https://doi.org/10.1080/1747423X.2017.1385653

Taylor & Francis
Taylor & Francis Group

ARTICLE

Predicting the effects of urbanization on runoff after frequent rainfall events

Noa Ohana-Levi[a], Amir Givati[b], Nurit Alfasi[c], Aviva Peeters[d] and Arnon Karnieli[a]

[a]The Remote Sensing Laboratory, Jacob Blaustein Institutes for Desert Research, Ben-Gurion University of the Negev, Sede Boker, Israel; [b]Surface Water and Hydrometeorology, Israeli Hydrological Service, Water Authority, Jerusalem, Israel; [c]Department of Geography and Environmental Development, Ben-Gurion University of the Negev, Beer-Sheva, Israel; [d]The Desert Architecture and Urban Planning Unit, Jacob Blaustein Institutes for Desert Research, Ben-Gurion University of the Negev, Sede Boker, Israel

ABSTRACT

Urbanization dynamics are commonly subjected to powerful market forces, only partly managed by land-use plans. The density, location and pattern of urbanized areas affect rainfall-runoff relations. Consequently, it is essential to understand future impacts of urbanization on runoff and produce focused regulation. The goal was to analyze land-cover scenarios and their impact on runoff in an urbanized watershed in Israel. Present and predicted land-cover scenarios in a densely populated watershed were produced. The runoff response to rainfall was then simulated using a hydrological model. The impact of implementing afforestation and quarrying national outline plans was considered. By the year 2050, 50% of the watershed will be urbanized with a linear increase in runoff response. Afforestation and quarrying plans show little effect on runoff, although quarries may decrease runoff through percolation. As urbanization is expected to continue spreading in adjacent watersheds, statutory measures should be applied to mitigating runoff.

ARTICLE HISTORY
Received 22 February 2017
Accepted 21 September 2017

KEYWORDS
Urbanization; watershed hydrology; remote sensing; land-cover projection

1. Background

Since the industrial revolution in the eighteenth century, urbanization has been the most intense form of land-cover change (LCC) in most developed areas (Orenstein, Bradley, Albert, Mustard, & Hamburg, 2011), with projections for the next decades pointing at continuing urban growth in developing countries (UN, 2014). This trend has affected and altered many ecological processes. The increase in impervious surface areas is a major driver of water-related problems and causes alterations in runoff response, such as increased frequency, speed and magnitude (W. Choi & Deal, 2008; Hong et al., 2012; Keppner et al., 2012). Additional processes accompanying urbanization also affect the hydrological response by increasing water availability to runoff. These include vegetation removal that leads to less canopy interception of rainfall, a decrease in ground cover, litter and debris, and a decrease in the loss of water due to evapotranspiration (Hernandez et al., 2000; Rulli & Rosso, 2007). In order to study land-cover (LC) impacts on hydrological aspects, a watershed-scale system that comprises an entire topographical unit draining into a single stream is preferred. Within the watershed, attempts have been made to quantify and understand the spatial and temporal variability and the patterns of LC types and to link them to runoff response (Ohana-Levi, Karnieli, Egozi, Givati, & Peeters, 2015). Hydrological regime alteration may be due to both LCCs and climate change effects (Hamdi, Termonia, & Baguis, 2010; Y. He, Lin, & Chen, 2013) and

CONTACT Arnon Karnieli karnieli@bgu.ac.il The Remote Sensing Laboratory, Jacob Blaustein Institutes for Desert Research, Ben-Gurion University of the Negev, Israel

adaptation measures to these changes are required in order to minimize their effects (Alley et al., 2003; Zahmatkesh, Karamouz, Goharian, & Burian, 2014). Climate change will most certainly have an impact on future rainfall regime and increase the risk of floods and the number of people exposed to floods (Black et al., 2008; Hirabayashi et al., 2013). There are short-term options for facing the problem of increased magnitude, frequency and intensity of surface flows that may be available through efficient planning and policy-making (Bates, Kundzewicz, Shaohong, & Palutikof, 2008).

The ability to anticipate changes in LC may assist in planning and management of urbanization processes (Zhang & Shuster, 2014). Moreover, projecting LCCs may provide a tool for assessing ecosystem change and environmental implications at both temporal and spatial scales (López, Bocco, Mendoza, & Duhau, 2001), including rainfall-runoff responses to rainfall events. Although present trajectories and trends may assist in simulating future LCCs, it is also essential to take into account the current and future land-use policy in the research area and to link it to possible impacts on runoff response.

Land-use policy serves as a tool for governmental bodies to achieve political objectives, and the spatial distribution of the population influences land-use priorities (Orenstein & Hamburg, 2009). Urban development is driven by factors such as population growth, economic processes, endogenous changes in the rural sector, and resource allocation. Planning policies formalized by governmental authorities and municipal agencies also need to account for land availability and environmental considerations (Shoshany & Goldshleger, 2002). The multi-dimensional nature of the built environment makes it difficult to control the details of urban expansion through statutory land-use planning, specifically in densely populated and continuously developing regions. Even when land-use is designated for specific areas, in many cases, a nonconforming development takes place (Alfasi, Almagor, & Benenson, 2012; Tian & Shen, 2011). There are several possible reasons for failure in applying statutory plans and for the necessity to introduce frequent local amendments to authorized plans. It may be the combination of a too detailed and too rigid land-use arrangement to fit the needs of rapid population and economic growth, and the fact that market forces and stakeholders play a major role as the initiators in a development-led system (Buitelaar, Galle, & Sorel, 2011; Tian & Shen, 2011; York et al., 2014). Moreover, since social and economic development are basically unpredictable, statutory plans are destined to be outdated or irrelevant soon after completion, and mostly reactive rather than guiding (Bramley & Kirk, 2005). Focusing the effort on specific values or on a defined location is, therefore, a more achievable goal.

In Israel, environmental land-use policy became crucial in the 1990s, as open space became a scarce resource (Orenstein & Hamburg, 2009). Open space preservation, in the context of ecological, recreational and aesthetic values, and the conservation of agricultural areas (mostly for their cultural-historical and aesthetic values, and not for their declining economic value) are mostly controlled and driven by governmental policy and are incorporated into land-use policies and national outline plans (NOPs) (Orenstein et al., 2011; Orenstein & Hamburg, 2009; Shachar, 1998). The weakness of NOPs in addressing the challenge of comprehensive, long-term protective policies raises the option of developing a hierarchy of necessities–that is, defining several critical key values and places that need protection, and focusing the efforts in safeguarding them by means of statutory planning.

The consequences of anthropogenic LCCs for runoff are still being studied (Baltas & Karaliolidou, 2008) and are important in the process of identifying the essential issues that should be taken into account during land-use planning. To consider sustainability in planning and decision making, the hydrological responses to projected LCCs must be illustrated (Keppner et al., 2012). Simulation models and tools for watershed planning and assessment provide a clear way to predict the effects of different LC scenarios that are the result of policy actions and management, for better practices and improvement of natural resource protection (Drescher et al., 2011; He & He, 2003; Keppner et al., 2012). After prediction, LC analysis is needed to consider future landscape structure and pattern and their evolvement in response to urbanization (Iovanna & Vance, 2007).

LC dynamics influence the hydrological regime continuously, while introducing a variety of spatial and temporal patterns and extents. Monitoring of LCC has been issued in many studies that dealt with effects on runoff response (Brabec, Schulte, & Richards, 2002; Dwarakish, Ganasri, & De Stefano, 2015; Ohana-Levi et al., 2015; Santillan, Makinano, & Paringit, 2011). A few studies focused on predicting runoff response to future LCC in varying temporal and spatial scales using methods such as Markov chain analysis, artificial neural networks and cellular automata (Deng, Zhang, Li, & Pan, 2015; Mahmoud, Alazba, & Chapman, 2015; Ongsomwang & Pimjai, 2015). However, relating to changes of patterns and composition as a result of planning strategies through time using spatial analysis and statistics are not very common in the literature. Simulations and quantifications of the hydrological effects of urbanization are highly documented in the literature. Different hydrological models are used for this purpose, such as the Soil and Water Assessment tool (SWAT) (Sisay, Halefom, Khare, Singh, & Worku, 2017), the Regional Hydro-Ecologic Simulation System (RHESSys) (Shields & Tague, 2015), Hydrologic Engineering Center – Hydrologic Modeling System (HEC-HMS) (Givati, Gochis, Rummler, & Kunstmann, 2016), and Weather Research and Forecasting Model (WRF-Hydro) (Gochis, Wei, & Yates, 2015). They benefit from the ability to input a wide range of parameters in order to simulate hydrographs for a given surface. The Israeli Water Authority (IWA) developed a local, uncoupled version of the WRF-Hydro model (Givati et al., 2016). It is a high-resolution, event-based hydrological forecasting model that relies on forecasted or measured rainfall data as input to simulate the hydrological response to rainfall. This model was used to study the effect of urbanization on runoff response following frequent rainfall events. Since it is an operational model used for management and policy-making purposes, it was found suitable for modeling urban and environmental planning scenarios.

The aim in the current study was to quantify and assess the future effects of probable urban development on rainfall-runoff relations for single rainfall events, in an urbanized watershed while addressing planning scenarios in future land-use policy. This aim was carried out by pursuing three specific objectives: (1) analyzing past, and future land-cover maps of the studied watershed, using satellite imagery; (2) simulating runoff volumes and maximum discharges for two rainfall events that are considered frequent, using different land-cover scenarios in the watershed; and (3) simulating runoff volumes and discharges while considering the implementation of different national outline plans.

2. Methodology

2.1. *Study area*

The research was conducted within the Ayalon watershed, located in Central Israel (Figure 1(a)). The watershed situated in a semi-arid climate zone with a mean annual precipitation of about 550 mm (Gvirtzman, 2002). The watershed is composed of three morphological units: mountainous, hilly and plain (Khavich & Ben-Zvi, 1995); the plain area contains the most densely populated region of the country, specifically, the Tel Aviv metropolis and some of its satellite cities (Rahamimoff, 2005). The watershed is politically divided between Israeli regions and West-Bank–Palestinian Authority (WB-PA); hence there were limitations to conducting extensive field research, resulting in the inevitable need for a remote sensing tool and LCC monitoring methods. The watershed has experienced extensive urbanization processes during the past decades, at the expense of agricultural and natural areas (AbuSada & Thawaba, 2011; Kliot, 1986). The most urbanized region within the watershed is the western plain unit, and there has been a continuous spread of built-up areas eastwards and uphill (Ohana-Levi et al., 2015).

The research area contains a wide array of LC and land-use types, some of which are still natural while most are controlled and managed. These include forests, different types of residential land-uses (high/low density, built/un-built areas, large cities, and villages), industrial areas, commercial areas, roads, grasslands, agricultural lands (row crops, orchards), and quarries. The research was

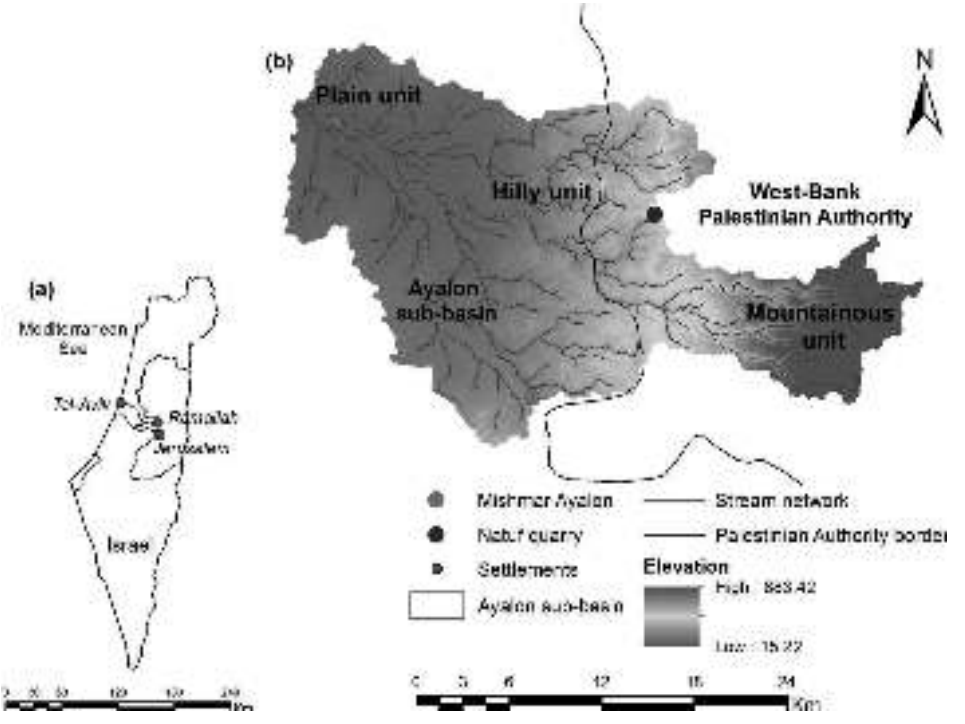

Figure 1. Study area of the Yarkon-Ayalon watershed (a) Within the area of Israel; and (b) The Ayalon-Ezra sub-basin that was studied.

conducted in the Ayalon sub-basin (Figure 1(b)) that was delineated according to the location of the hydrometric station downstream. In 1957, a reservoir named Mishmar Ayalon was built at the eastern hilly part of the sub-basin, in order to minimize the peak discharges during severe flooding events, and has never experienced an overflow by floodwater. This has reduced the effective area of the catchment (Khavich & Ben-Zvi, 1995). Therefore, the Mishmar Ayalon drainage area was excluded from the Ayalon sub-basin's area. Additionally, in the mid-2000s, a large quarry was established in the northeastern hilly part of the watershed, with ponding and percolating runoff flows reaching it. This quarry's drainage area was also excluded from the Ayalon sub-basin, reducing it to a total drainage area of 538 km^2 (Figure 1(b)).

2.2. *The LCM model*

The LCM is an extension for Geographic Information System (GIS) software packages. It is designed to analyze past LCCs, to model the potential for land transitions and future change, to predict the phenomena's evolution and the course of change into the future, and to integrate planning regimes and interventions into prediction (Paegelow, Olmedo, & Camacho, 2008; Ronald, 2006). In the current study, the Multi-Layer Perceptron (MLP) neural network algorithm was used to model transitions between the different LC classes. MLP is capable of modeling complex relationships between variables and is therefore suitable for this study. In order to model the transition potential, the model requires a set of explanatory variables (Mishra, Rai, & Mohan, 2014), provided by the user. The model then calculates Cramer's Coefficient for each explanatory variable, indicating the degree to which it is associated with the distribution of the LC classes. The variables that contribute most to the explanation of the LC spatial distribution are selected for the model simulation (Pérez-Vega, Mas, & Ligmann-Zielinska, 2012).

Based on the 2003 and 2014 satellite-derived LC maps (described in Section 2.4) along with the explanatory variables, the transitions are modeled using MLP neural networks. The transition potential outputs include values between 0 and 1 for each pixel and express the potential of change between each the different LC types per pixel. The MLP relies on transition sub-models that consist of one or more LC transitions and have the same underlying drivers. For examples, transitions from bare soil to urban LC and from row crops to urban LC, are thought to have the same driver, which is urbanization. The model then links the transitions and explanatory variables and derives potential change maps for each transition (Pérez-Vega et al., 2012). A location is more vulnerable to change if it is prone to several transitions. A hard-classification map is created when the model determines the pixels with the greatest potential for the occurrence of a specific LCC (Camacho Olmedo, Paegelow, & Mas, 2013).

The model also enables taking into account incentives and constraints to limit the LCC in specific areas. Values are given to these specific locations, where 1 represents no effect of constraints, a value >1 increases transition potential, a value < is a disincentive and 0 is an absolute constraint (Figure 2). The LCM was used to create four LC prediction maps, for the years 2020, 2030, 2040 and 2050.

2.3 *The uncoupled WRF-hydro model*

The uncoupled WRF-Hydro model is a stand-alone uncoupled version of the original WRF-hydro (Fredj, Silver, & Givati, 2015; Gochis et al., 2015). It is a physical event-based model aimed at simulating hydrographs for specific rainfall events while capturing spatial distribution of input meteorological variables and physical parameters. It integrates measured rainfall data that is based on the Israeli Meteorological Service (IMS) database and is interpolated to a 3 km grid using the inverse distance weighting procedure (Givati et al., 2016) in order to create a continuous surface of rainfall values within the watershed. The model is simulated using spatial analyses in a GIS software package to provide short-range hydrological simulations. This is implemented through toolboxes that are used for receiving input parameters and variables. The model outputs include a specific runoff value at locations along the watershed, as well as a watershed hydrograph.

Calibration of the model relies on partitioning the amount of water that infiltrate into the soil versus the portion that flows as runoff, to determine the water movement into channels. Overland flow routing parameters determine the speed of water movement across the landscape and in channels. Rougher surfaces slow down the flow towards the channels and during this time the chance of water infiltration into the soil increases. Therefore, the roughness coefficient determines both the timing and amount of flow (Givati et al., 2016). Soil hydraulic parameters are a function of soil types and LC and are evaluated empirically. The calibration process was conducted by adjusting the Manning roughness and runoff coefficients, and comparing four simulated hydrographs of frequent storm events in recent years (2012 and on) to measured maximum runoff discharge and volume values. If the bias between the compared variables was > 25%, the runoff coefficients were adjusted and the comparison was carried out once again. In addition, the Nash–Sutcliffe model efficiency (NSE) coefficient was used to assess the overall performance of the model (Nash & Sutcliffe, 1970). The calibration process was performed using the 2014 LC map, in order to comply with the time periods of the selected rainfall events for calibration. LC is rapidly changing in the Ayalon sub-basin, and therefore the rainfall events that were used for calibration and validation of the model were limited to 3 years prior and after the 2014 image was acquired.

A rainfall event that has a recurrence time of < 50% and occurs at least once in two years is considered frequent. Two rainfall events, specified in Section 2.5, with a recurrence time <50%, were used to operate the model. The decision to use frequent events was based on different studies that found low variability of runoff response during extreme runoff events between different land-cover types (pervious and impervious)(Guan, Sillanpaa, & Koivusalo, 2016; Ohana-Levi et al., 2015). The study focused on enhancing the distinction between the LC types' reaction to rainfall, and using frequent rainfall events enabled this

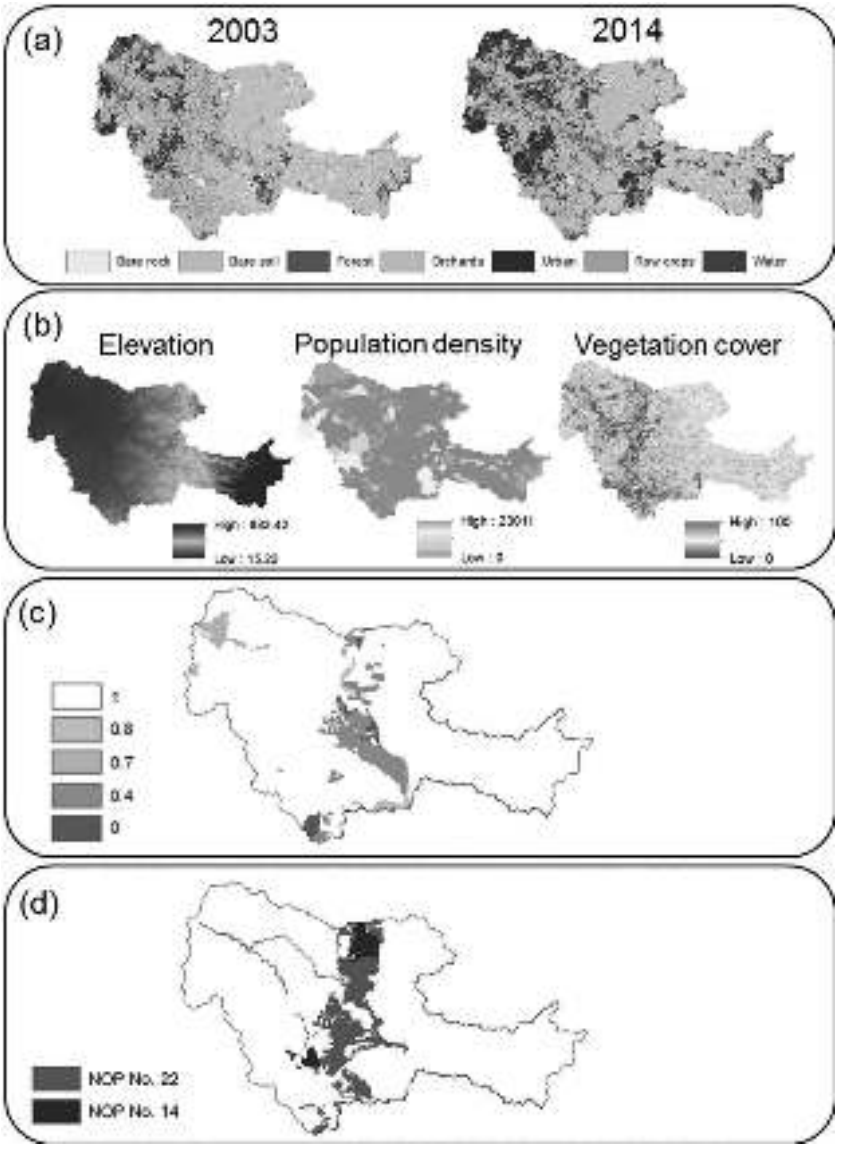

Figure 2. Inputs to the LCM model: (a) Land-cover maps for 2003 and 2014; (b) Explanatory variables, including elevation (m), population density (individuals/km^2), and vegetation cover; (c) Constraints; and (d) National Outline Plans (NOP No. 14: mines and quarries, NOP No. 22: forest and afforestation).

comparison. Each rainfall event was simulated using all LC maps (2003 to 2050), so that eventually there were six different simulations for each rainfall event. This was performed in order to learn how the LCC process during five decades affected frequent rainfall-runoff response.

In order to study the third specific objective and understand the possible effects of applying the NOPs, layers representing two plans were overlaid on the 2020 LC map and used as inputs to the hydrological model. The first was NOP No. 22 for forest and afforestation, and the second was NOP No. 14 for mining and quarries. This procedure was carried out to study three different scenarios: (1) the forest and afforestation NOP was overlaid on the 2020 LC map; (2) the mining and quarrying NOP was overlaid; (3) the mining and quarrying NOP was overlaid, but this time assuming that the quarries were designed to pond and percolate the runoff flows that reach them.

2.4. *Data sets used as inputs for the LCM model*

The LCM model requires several input data sets to simulate future LCC predictions (Figure 2):

(a) LC maps. Classified maps based on satellite imagery that were acquired on 7 February 2003 and 13 February 2014 from Landsat 7 Enhanced Thematic Mapper (ETM) and Landsat 8 (OLI), respectively, with a spatial resolution of 30 m. Following pre-processing, the images were classified using the maximum likelihood classification technique (Arbia, Benedetti, & Espa, 1999) to seven different LC classes: bare soil, orchards, water, row crops, bare rock and urban. Then, an accuracy assessment procedure was conducted against a high resolution orthophoto in order to evaluate the certainty of the final classification maps (Foody, 2004). For validation of the LCM results, a Landsat Thematic Mapper (TM) image acquired on 30 January 2009 was pre-processed and classified using the same techniques mentioned above. It was used along with the 2003 classified image in the LCM model to predict a LC map for 2014. Then, the comparison between the 2014 LC maps (classified vs predicted) was calculated based on percent coverage of each LC class within the sub-basin.

The prediction of future LC maps relies on providing a suitable trend or trajectory of LCC. There are many forces that may alter the course and dynamics of the LCC trend; however, in this study, the focus was on a future scenario in which the current direction of the development and spread of urban cover will proceed at a similar rate. The national LCC trend between 2003 and 2014, used as the basis for the LC projection (Figure 2(a)), is based on the medium growth-rate scenario of population according to the Israeli Central Bureau of Statistics (Weisthal, 2014), in which the tendency of both construction and population growth since the early 2000s is relatively constant in its direction and magnitude.

(b) The LCM requires the use of explanatory variables. After testing many possible explanatory variables, the three most powerful were chosen as inputs to the model. These included elevation, represented by a digital elevation model (DEM), population density, based on both the Israeli and Palestinian central bureaus of statistics, and vegetation cover, represented by a Normalized Difference Vegetation Index (NDVI) (Sonwalkar, Fang, & Sun, 2010) that was produced from the 2014 Landsat 8 OLI image (Figure 2(b)).
(c) Strict constraints regarding future development, based on current management policy, were defined for parts of the study area. Areas defined in official district plans, such as national parks, forests, possible future national parks, nature reserves, metropolitan parks, and major city parks, were labeled as disincentives for future change. Their transition potentials were decreased, and they were given different constraint levels (Figure 2(c)). Future predictions referred to these locations as less probable to be transformed. The data regarding these constraints were derived from the Planning Administrations of the Tel-Aviv and Central Districts.
(d) GIS layers of the two chosen NOPs included forests and afforestation (approved in Nov. 1995, last changed in Oct. 2013) and mining and quarrying (approved in Jan. 1998, last changed in May 2013). Both layers are based on data from the NOPs, Israeli Planning Administration, Ministry of Finance (Figure 2(d)).

2.5. *Data sets used as inputs for the uncoupled wrf-hydro model*

The uncoupled WRF-Hydro hydrological model requires several input data in order to operate it, described in detail below (Figure 3):

(a) A layer of the Ayalon sub-basin domain (Figure 3(a)).
(b) A soil-type raster from the Survey of Israel and a LC raster map, along with tabulated empirically based runoff coefficients for each soil type and LC type (Figure 3(b1,b.2,c).

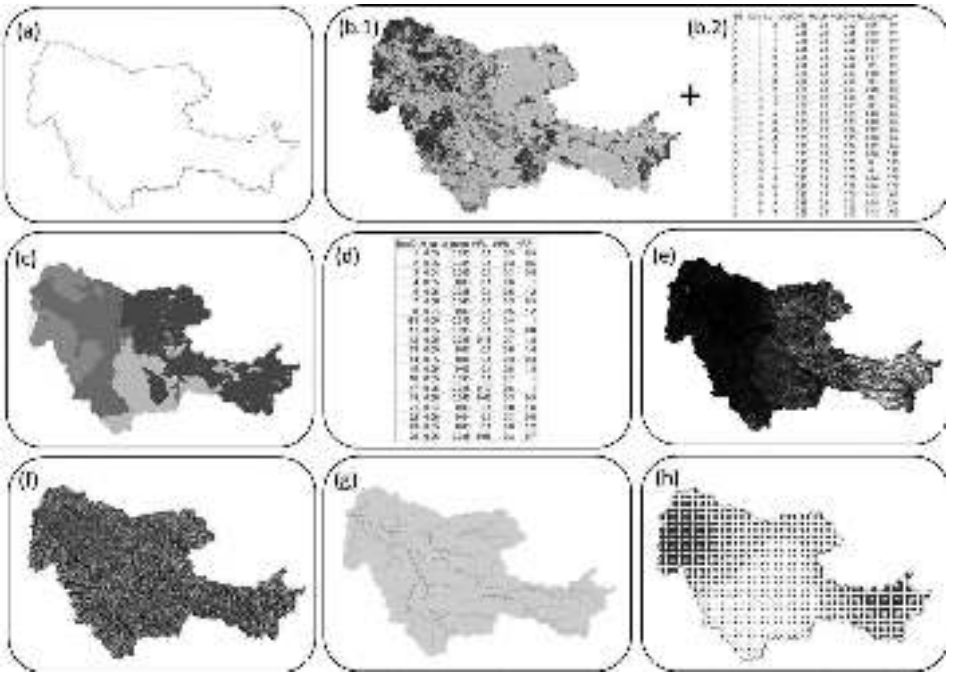

Figure 3. Inputs to the uncoupled WRF-Hydro model: (a) Watershed domain; (b.1) Land-cover map; (b.2) Runoff coefficients table; (c) Soil map; (d) Manning coefficients table; (e) Slopes; (f) Flow direction; (g) Flow accumulation; (h) Interpolated rainfall for the storm events based on meteorological measurements; larger sized samples denote larger amounts of rainfall.

The runoff coefficients table includes coefficients for 9 different LC types that comply with the research design and the LC maps. The LC maps used for this model are the products of the Landsat classified images and the LCM model prediction maps, as specified in Section 2.2.

(c) Manning roughness coefficients and a hydraulic radius table, calculated for this specific sub-basin (Figure 3(d)). The Manning roughness coefficients are based on measurements from the hydrometric stations, conducted by the IWA.

(d) Slope, flow direction and flow accumulation maps derived from a DEM (Figure 3(e,f,g).

Measured rainfall data, interpolated for the entire sub-basin area (Figure 3(h)), and soil moisture calculated values. The rainfall events that were chosen for this study took place from Dec. 20-23, 2014, and Apr. 11-13, 2015, with a spatially weighted total average of about 17 and 27 mm of rain, respectively. These events are considered frequent and have a recurrence time >50%, meaning that events of this magnitude occur almost every year and are more commonly impacted by LCC. The rainfall data was selected from the IMS website and was based on measurements from 8 rainfall gauges within and near the Ayalon sub-basin.

2.6. *Data analyses*

LCC was analyzed by comparing the six LC classes (the water LC class was omitted from the analyses due to its very low coverage) of the six LC maps to each other. The percent of the sub-basin that each LC class covered in every time step was calculated and the differences were compared. Moreover, a regression model was applied for each LC class to observe the relations between areal cover (km^2) and time. Only significant relations (p-value ≤ 0.05) were considered.

The hydrological model output hydrographs for each LC map were plotted together for every rainfall event in order to observe the differences in discharge. The total runoff volume values for each time step were also compared. In addition, the percent of change was calculated for both maximum discharge and runoff volume between each pair of subsequent LC maps. Also, a regression model was applied for each of the LC classes' areal coverage against the maximum discharge and runoff volume for each rainfall event. This was implemented in order to evaluate the impact (significance and relationship strength) through time that each LC type had on each of the hydrological variables.

The hydrological model was also applied using the 2020 LC map with the overlaid NOPs. This model's output results for each of the overlaid maps was compared against the hydrograph that was derived using the original 2020 LC map in order to study the possible differences in discharge. In addition, the percent of change was calculated for the hydrological variables while using the 2020 LC map and each of the NOP maps as inputs for the hydrological model.

3. Results

3.1. *Generating the LC maps*

Two Landsat classified images were used as inputs for the LCM model, representing the recent trend in LCC in the Ayalon sub-basin. These satellite-derived images were acquired in 2003 and 2014 and classified to seven LC classes (Figure 2). The accuracy assessment for these images showed a total accuracy of 87.43% and 88.56% for the 2003 and 2014 maps, respectively. The 2009 classification map that was used for validation of the LCM, had a total accuracy of 92.57%.

The validation comparison between the classified and prediction 2014 maps was performed for each class separately, and the errors ranged between 14.4% and 45.38% (after ignoring the water LC class, as specified in Section 2.6).

The future prediction maps that were generated using the LCM were based on the 2003 and 2014 satellite-derived classified maps (Figure 2(a)). The future maps forecast a sharp increase in urban areas over the studied time period (Figure 4). The results show that if the current LCC trend continues, by 2050 almost 50% of the Ayalon sub-basin will be covered by an urban landscape. At the same time, the area that is covered by bare soil and orchards will continue to gradually decrease so that by 2050 bare soil and orchard coverage will decrease by 50%. The bare rock LC type does not change much over time, since it mostly characterizes areas that are going through urbanization. This means that areas covered with bare rock will soon be covered by an urban LC type. Forests and row crops are undergoing a moderate decrease, since they are mostly defined as conservation areas; thus, the majority of these LC types will be preserved (Figure 5).

Row crops and forests showed non-significant change through time since they were constrained while applying the LCM simulations. For bare rock, the relationship of areal coverage against time was not strong ($R^2 = 0.67$). Bare soil, orchards and urban LC types show significant and strong linear relations with time (R^2 values ranging between 0.86 and 0.98). The slope coefficient of the urban LC points at a growth rate of 4.8 km^2 a year. An opposite trend is apparent in the bare soil and orchard LC types, with an annual decrease in areal cover of 2.28 and 2.1 km^2, respectively.

3.2. *Hydrological model*

The model calibration included the use of six different frequent rainfall events between Feb. 2012 and Nov. 2014, in order to be suitable for the 2014 LC map, used as an input to the

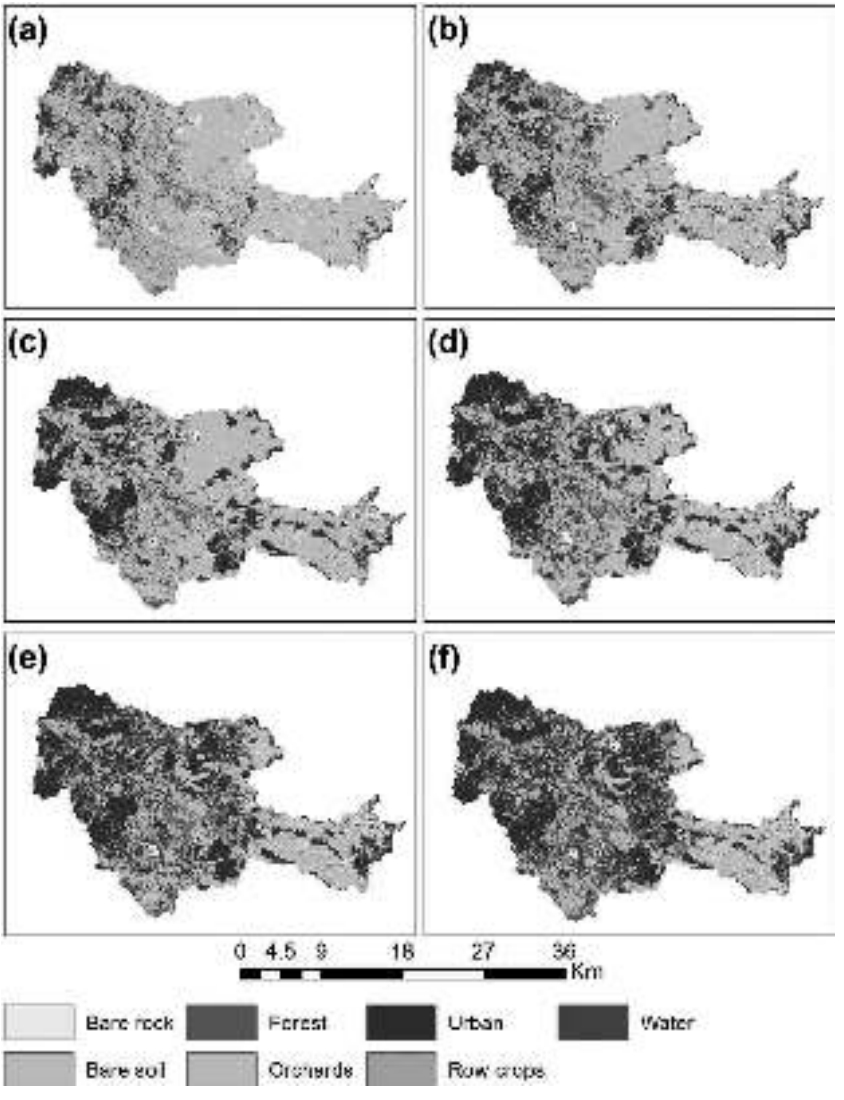

Figure 4. Two classified Landsat images of the years (a) 2003 and (b) 2014, and predicted land-cover maps for the years (c) 2020, (d) 2030, (e) 2040, and (f) 2050.

model (Table 1). The results were compared to the measured hydrographs using the NSE coefficient. The NSE varied between −1 and 0.88, with most of the events scoring > 0.4. The rainfall events that were used for the analysis had NSE of 0.66 and 0.82 (Table 1). Most of the validation results show less than 25% difference between simulated and measured maximum discharge and runoff volume.

The change in LC through time was linear and rapid, and correspondingly, the hydrological response also represented a linear increase between 2003 and 2050 (Table 2, 3, Figure 6). For runoff volume and maximum discharge through the years for the Dec. 20–23, 2014 event, the R^2 values were 0.98 and 0.88, respectively. For runoff volume and maximum discharge through the years for the Apr. 11–13, 2015 event, both R^2 values were 0.99. .

A regression statistical analysis was conducted in order to check for a relationship between the different LC types and the runoff response. Both maximum discharge and runoff volume were analyzed against LC type areal coverage through time (Table 4). The results for both rainfall events

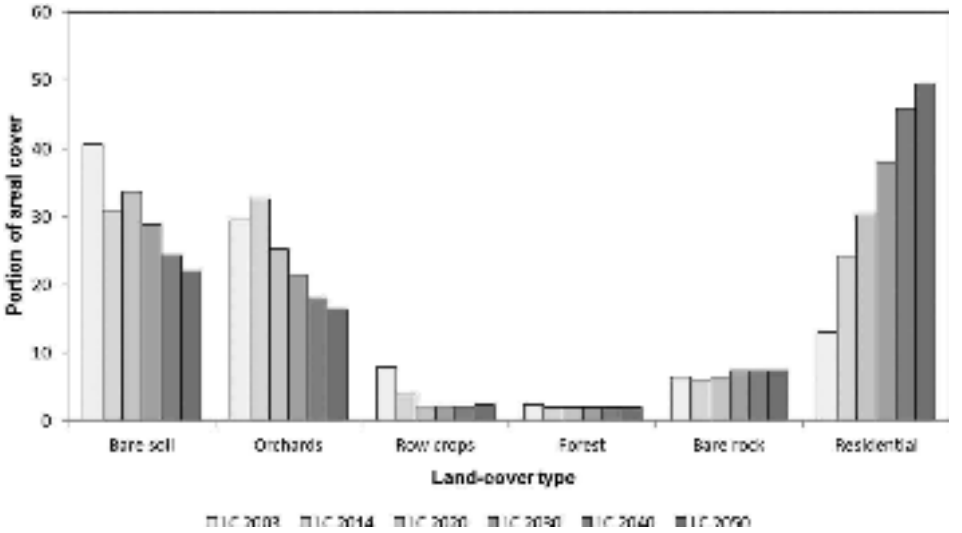

Figure 5. Portions of the areal coverage of each land-cover type (LC) in each of the classified and predicted land-cover maps.

Table 1. Rainfall events used for calibration, validation and analysis, along with their runoff volume and maximum discharge values, as measured by the hydrometric station.

	Rainfall events by dates	Maximum discharge (m^3/sec)	Runoff volume (1 million m^3)	Maximum discharge percent difference	Runoff volume percent difference	NSE
calibration	October 31 – 5 November 2014	28.37	1.81	17.49	11.01	−1.02
	November 16–17, 2014	57.65	1.63	−22.85	−19.42	0.86
	December 20–22, 2012	45.5	2.44	−58.97	−12.54	0.44
	April 17–23, 2013	23.79	0.69	12.15	35.67	−1.05
	November 09–12, 2012	28.76	2.95	−6.27	−16.47	0.14
	December 13–15, 2014	18.25	0.62	24.40	15.16	0.58
validation	February 18–22, 2015	25.34	2.70	21.52	−8.20	0.33
	April 3–5, 2011	29.15	0.57	−7.98	36.54	−0.01
	January 1–2, 2012	44.45	1.46	−25.29	23.10	0.88
analysis.	April 11–13, 2015	17.5	0.97	41.62	−26.03	0.66
	December 20–23, 2014	22.86	0.80	22.28	−1.89	0.82

show significant relations between all LC types, except row crops. The urban LC type showed much stronger relations than the rest of the LC types, with R^2 values between 0.93 and 1.

3.3. *Implementation of national outline plans (nops)*

The locations of forests and afforestation and mining and quarrying NOPs were overlaid on the 2020 LC map (Figure 7). The results of the hydrological model, using these NOP maps as inputs, show quite negligible changes (Table 5). The effect forest and afforestation on the runoff response for the two rainfall events, compared to the results of the model with the original 2020 LC map, was a decrease of up to 2.5% in runoff volume and 3.2% in the maximum discharge. For mining and quarrying, the model simulations show almost no change. However, when simulating a scenario of ponding and percolating runoff flows that reach the quarries, similar to the quarry that already exists in that area, the results indicate a very significant decrease in the runoff response. For runoff volume and maximum discharge, the simulations show up to 14.10% and 11.23% decreases, respectively.

Table 2. The amount of maximum discharge, runoff volume, percent areal cover for each land-cover type and the percent change for each classified/predicted period, for the December 20–23, 2014 rainfall event.

	Value for each land-cover map					
	2003	2014	2020	2030	2040	2050
Maximum discharge (m^3/sec)	20.64	29.41	37.34	46.99	47.43	47.80
Runoff volume (1,000,000 m^3)	0.53	0.76	0.93	1.16	1.33	1.40
Bare soil percent areal cover	40.68	0.31	0.34	0.29	0.24	0.22
Orchards percent areal cover	29.45	32.65	25.32	21.51	18.06	16.42
Row crops percent areal cover	7.93	3.89	2.15	2.18	2.21	2.48
Forest percent areal cover	2.40	2.03	2.03	2.03	2.03	2.03
Rock percent areal cover	6.48	6.16	6.51	7.47	7.45	7.37
Urban area percent areal cover	13.02	24.29	30.31	37.97	45.87	49.63
	Percent change between consecutive years					
	2003–2014	2014–2020	2020–2030	2030–2040	2040–2050	
Maximum discharge	29.85	21.22	20.55	0.91	0.79	
Runoff volume	30.04	18.24	19.83	12.67	5.06	
Bare soil	−29.00	−19.43	−18.18	−10.18	−6.60	
Orchards	7.34	−2.63	−6.84	−9.58	−7.96	
Row crops	−122.59	−74.20	−72.25	2.83	11.62	
Forest percent	1.85	−0.06	0.00	0.00	0.00	
Rock	13.88	8.38	19.34	2.87	0.93	
Urban	49.92	26.54	16.37	12.96	8.17	

Table 3. The amount of maximum discharge, runoff volume, percent areal cover for each land-cover type and the percent change for each classified/predicted period, for the April 11–13, 2015 rainfall event.

	Value for each land-cover map					
	2003	2014	2020	2030	2040	2050
Maximum discharge (m^3/sec)	21.20	29.98	35.65	44.52	53.00	57.27
Runoff volume (1,000,000 m^3)	0.82	1.16	1.45	1.74	2.04	2.17
Bare soil percent areal cover	40.68	0.31	0.34	0.29	0.24	0.22
Orchards percent areal cover	29.45	32.65	25.32	21.51	18.06	16.42
Row crops percent areal cover	7.93	3.89	2.15	2.18	2.21	2.48
Forest percent areal cover	2.40	2.03	2.03	2.03	2.03	2.03
Rock percent areal cover	6.48	6.16	6.51	7.47	7.45	7.37
Urban area percent areal cover	13.02	24.29	30.31	37.97	45.87	49.63
	Percent change between consecutive years					
	2003–2014	2014–2020	2020–2030	2030–2040	2040–2050	
Maximum discharge	29.29	17.35	18.53	16.00	7.46	
Runoff volume	29.38	16.54	20.18	15.00	5.73	
Bare soil	−29.00	−19.43	−18.18	−10.18	−6.60	
Orchards	7.34	−2.63	−6.84	−9.58	−7.96	
Row crops	−122.59	−74.20	−72.25	2.83	11.62	
Forest percent	1.85	−0.06	0.00	0.00	0.00	
Rock	13.88	8.38	19.34	2.87	0.93	
Urban	49.92	26.54	16.37	12.96	8.17	

4. Discussion

4.1. *The dynamics of LCC*

The aim of the first specific objective was to analyze the past, present and predicted LC maps of the sub-basin under question. The final LC maps have inherent errors caused by the classification process and the LC projection procedure. LC modeled in a 30-m resolution will suffer from uncertainty due to mixed pixels, topographic effects and spectral confusion of LC types (Irons et al., 1985; Moody & Woodcock, 1995). In addition, the projections assume a similar trend of LCCs

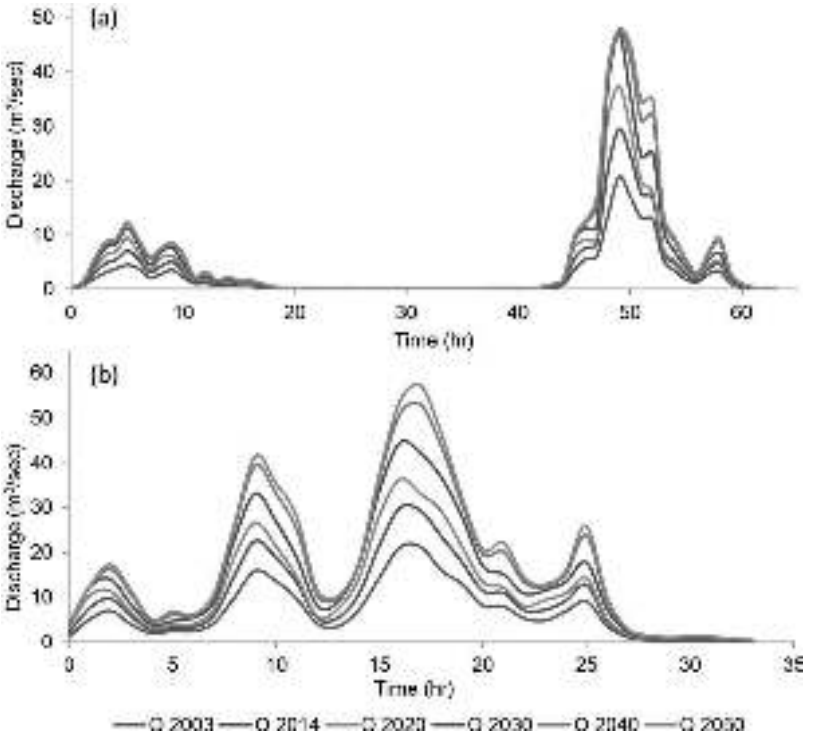

Figure 6. Hydrographs for two frequent rainfall events: (a) December 20–23, 2014; and (b) 11 April 2015. For every rainfall event, the uncoupled WRF-Hydro model was applied using all land-cover maps.

Table 4. The relationship between each of the land-cover types and the maximum discharge and runoff volume for the two rainfall events. The relationship strengths are represented by R^2 values.

	Dec. 20–23, 2014		Apr. 11–13, 2015	
Land cover	R^2	p-value	R^2	p-value
Maximum discharge regressions				
Bare soil	0.79	0.02	0.90	0.00
Orchards	0.80	0.02	0.88	0.01
Row crops	0.77	0.02	0.60	0.07
Bare rock	0.73	0.03	0.71	0.03
Urban	0.93	0.00	1.00	0.00
Runoff volume regressions				
Bare soil	0.89	0.00	0.90	0.00
Orchards	0.87	0.01	0.88	0.01
Row crops	0.65	0.05	0.61	0.07
Bare rock	0.73	0.03	0.73	0.03
Urban	1.00	0.00	1.00	0.00

as calculated for the past decade, relating to a linear trend, hence the LC maps used for the analyses should be considered as a possible proxy for future scenarios. The results reflect the rapid and accelerated trend of growth in urbanization cover in the past and projected future until the year 2050. In 2003, only 13% of the sub-basin's area was covered by urban LC and future forecasts show an increase of up to 50% coverage of the Ayalon sub-basin by an urbanized landscape. The expansion of built-up LC in the past and the future occurs at the expense of other LC types, mainly bare soil, orchards and row crops. In total, according to the projected trend, about 37% of the sub-basin's area will be transformed from bare soil, orchards and row crops to urbanized cover by the

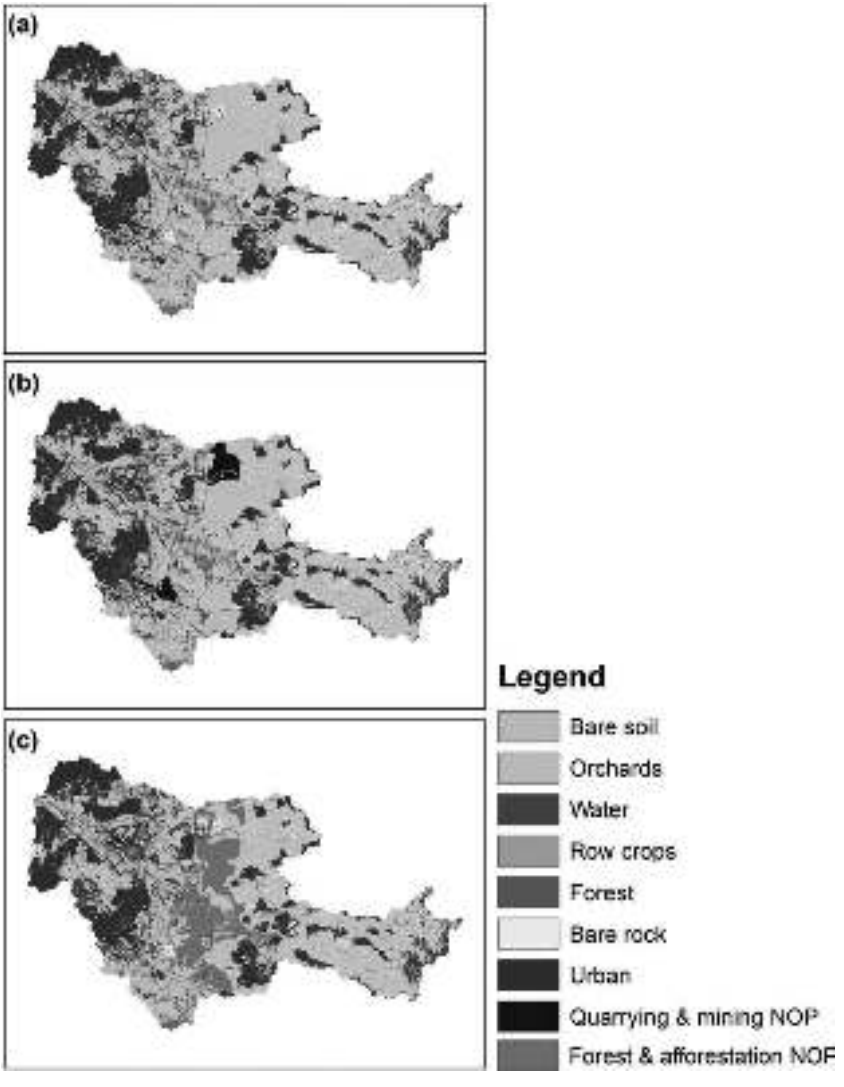

Figure 7. Land-cover maps of (a) prediction status of year 2020; (b) map of 2020 with the quarrying and mining master NOP; and (c) map of 2020 with the forest and afforestation NOP integrated.

year 2050, with an average annual urban growth of 4.8 km^2. These high rates of urbanization located in the low-elevation area of the sub-basin correspond to other studies that demonstrate that coastal zone areas are more prone to urbanization than any other morphological unit in a watershed (Fragkias & Seto, 2012; Neumann, Vafeidis, Zimmermann, & Nicholls, 2015; Seto, Fragkias, Guneralp, & Reilly, 2011).

4.2. *The hydrological model performance*

In this study, the uncoupled WRF-Hydro model was used as a research tool for the first time. The NSE scores showed a good performance for most calibration and validation events; however, the ratio between measured and simulated runoff volume and maximum discharge were of a higher importance, since this study aimed to study the effect of urbanization on these factors. In most cases, the accuracy was around 75% or higher, which indicated on a satisfactory performance for a

Table 5. Results of the hydrological simulations after using the national outline plans (NOPs) as inputs. NOP quarries (a) and NOP ponding quarries (b) relate to different scenarios of implementing the mining and quarrying NOP: (a) relates to a scenario in which the quarries are established and classified as bare rock and (b) simulates a scenario of ponding and percolating runoff water that reaches these quarries.

	Dec. 20–23, 2014			Apr. 11–13, 2015		
	2020 LC	2020 NOP Forests	% change	2020 LC	2020 NOP Forests	% change
Maximum discharge (m^3/sec)	38.90	37.70	−3.2	35.66	34.88	−2.23
Runoff volume (10,000 m^3)	96.66	94.36	−2.43	144.37	140.84	−2.5
Relative forest cover (%)	2.03	10.97	81.5	2.03	10.97	81.5
	2020 LC	**2020 NOP quarries (a)**			**2020 NOP quarries (a)**	**% change**
Maximum discharge (m^3/sec)	38.90	38.94	0.26	35.66	35.77	0.30
Runoff volume (10,000 m^3)	96.66	96.91	0.10	144.37	144.74	0.25
	2020 LC	**2020 NOP ponding quarries (b)**			**2020 NOP ponding quarries (b)**	**% change**
Maximum discharge (m^3/sec)	38.90	37.95	−2.52	35.66	32.06	−11.23
Runoff volume (10,000 m^3)	96.66	87.38	−10.62	144.37	126.53	−14.1

study that is conducted on a rather coarse scale. Future improvements to the model include the ability to produce a hydrograph at any point along the channel, an automatic calibration system based on corrected radar rainfall data, and a larger variety of rainfall inputs such as radar and an ensemble of meteorological models.

4.3. *Runoff response to LCCs*

In this study, each of the six LC maps was used as an input to the hydrological model. Both the maximum discharge and runoff volume values show a gradual, linear increase between 2003 and 2050, a trend that corresponds to the linear increase in urban LC. In general, urban growth is linked to shorter concentration time resulting in a shorter time to peak discharge (Nirupama & Simonovic, 2007). However, Figure 6 shows no such change. One reason for this is that smaller, more frequent rainfall events with low magnitudes such as in this study, only affect the runoff amount that experiences change, and do not have an impact on the concentration time (Guan et al., 2016). Other studies found that in highly urbanized watersheds there is little or no change in time to peak discharge, regardless of the increase in peak discharge and runoff volume (Chen, Youpeng, & Yin, 2009; Miller et al., 2014). This could also be a result of model limitations. Since the uncoupled WRF-Hydro model is a local development and is continuously upgraded and improved, this issue is also tested and will be addressed in future versions of the model.

Regression coefficients were calculated to understand the relations between each of the LC types' areal coverage and the runoff variables. This study has found significant relations between all LC types, except crops and forest, and runoff response. The strongest relations belong to the urban LC type for both rainfall events. This means that reducing the areal coverage of bare soil and orchards at the rates presented in this study in favor of urbanization processes is likely to result in increased runoff response, as shown in previous studies (Jacobson, 2011).

Future urbanization growth is expected to affect other hydrological and environmental aspects in the Ayalon sub-basin. These include an impact on the quantity and quality of groundwater; urban construction creates more impervious surface, reducing infiltration and available water for groundwater discharge (Carmon, Shamir, & Meiron-Pistiner, 1997). The quality of water is affected by urban land use, with a documented increase in pollutants such as chlorides, nitrates and heavy

metals, mostly from sources such as septic tanks, leaks in sewage collecting systems, landfills and solid waste, vehicles and fuel depots and more (Carmon et al., 1997; B.-Y. Choi et al., 2005). Also, With higher runoff volumes and peak discharges as a result on ongoing urban expansion, sediment yield from channel erosion is expected to grow (Trimble, 1997).

4.4. *NOP implementation*

As shown in many studies in the past, afforestation plays a significant role in regulating surface runoff through mechanisms such as canopy interception, evapotranspiration, litter fall interception and infiltration (Munoz-Villers & McDonnell, 2013; Yu, Wang, Coles, Xiong, & Xu, 2015). In this case study, implementing the forest and afforestation NOP No. 22 on the 2020 LC scenario resulted in a minor decrease in runoff simulations for the Ayalon sub-basin, with a decrease in streamflow of around 2.5%. The planned forests, according to the NOP, will be located on the hilly part of the Yarkon-Ayalon sub-basin, east of the plain area, which contains the majority of the population and urbanized coverage. Thus, the reduction of surface water that is expected to result from enlarging the forested area will only affect runoff from the upper part of the sub-basin, where urbanization processes are expected to be quite moderate. The plain area that is expected to experience most of the urban increase will not be affected by the afforestation NOP at all.

Quarries and bare rock areas may have an increasing effect on rainfall-runoff relations (Darwish et al., 2011). In this study, the findings show that the designated quarries, according to the mining and quarrying NOP, will occupy an area of 19 km^2, which constitutes 3.5% of the Ayalon sub-basin area. The locations assigned to these quarries, according to the NOP and the 2020 LC scenario, are projected to be covered with bare soil, row crop and orchard LC types if the NOP is not executed. The hydrological model simulation shows no change in runoff response compared to the projected 2020 LC scenario. The second quarrying and mining NOP scenario relates to the possibility of ponding and percolating the water flow that reaches these quarries, thus preventing the area that drains to the quarries from contributing runoff to lower parts of the watershed. Such drainage solutions and many others are being practiced around the world in various techniques and quarries (County-of-Santa-Cruz-Planning-Department, 2009; Miralles, García-Sánchez, & Jordán, 2006). In this scenario, the reduction in water flow is significant, with between 2.5 and 14% decreases in runoff response. This illustrates the role that applying NOPs can play in affecting environmental practices.

As reviewed before, when dealing with urban development, NOPs are shown to be less effective under strong external forces and pressures that take place in the process. In many cases of developing urban areas, the dynamics involved in urban development are too rapid and fast for the NOPs to be relevant and absolute, and manage the metropolitan expansion in a sustainable way (Kotter, 2004; Pauchard, Aguayo, Pena, & Urrutia, 2006). The Ayalon sub-basin is also politically divided between the Israeli and Palestinian authorities, creating a highly complicated situation for treating the watershed as one landscape unit while planning. Urbanization processes are no longer typical only for the growth of cities, but influence the dynamics in the rural countryside as well. Urban development is responsible for processes such as residential and industrial land development, as well as infrastructure outside the core of the cities, inducing expansion and different patterns of urban forms (Antrop, 2004). The expected expansion of the urban landscape might not be compatible with current NOPs, while plans addressing environmental features such as forests are shown to be ineffective in contributing to minimizing climate change and urbanization effects in the Ayalon sub-basin. Thus, placing the forested LC in the hilly part of the watershed, as determined by the NOP, will not succeed in regulating major portions of the runoff in the watershed.

The current rate of urban development highlights the urgent need for a feasible, cost-effective, sustainable solution for the subsequent increase in surface runoff. Since NOPs are most likely ineffective in meeting the needs of runoff mitigation, perhaps water-sensitive planning and runoff harvesting should be considered within urban areas (Shamir & Carmon, 2007). These include micro

and mesoscale interventions for sustainable local projects, as part of regional master plans. Some of these projects include integrating transportation planning. Others consist of urban runoff best management practices (BMPs) such as ponding and/or infiltrating surface water into groundwater closest to the source; at the microscale level, these include special constructions within buildings' yards, private gardens, playgrounds, etc. (Lovinger, Nardy, & Malka, 2013; Shamir & Carmon, 2007), or at the mesoscale level, within a neighborhood, using traffic circles that collect water, green roofs and biofilters (Tal, 2015). These measures have already been successfully implemented in parts of Australia, England, the USA, Canada and other countries, and three biofilters are currently operating efficiently in two different cities in Israel. Percolating runoff water into groundwater is also being implemented within and outside urban areas (Shamir & Carmon, 2007; Tal, 2015).

It is well documented that new forms and the development of transportation stimulate urbanization processes (Antrop, 2004; Behan, Maoh, & Kanaroglou, 2008) and may induce decentralization effects and expansion to the metropolitan fringe (Israel & Cohen-Blankshtain, 2010). The focus of this paper was on a specific, highly populated, dense sub-basin in the center of Israel; however as transportation and infrastructure improve and mobility options develop spatially (more train railways, better access to highways, a new light rail currently being built in the central district), it is expected that more areas in Israel will be affected and more watershed areas will experience massive urban development and LCC, leading to a more homogeneous landscape. It has been shown that increases in impervious cover for rural watersheds may introduce a greater impact on maximum discharges and the duration of floods than for existing urban areas (Miller et al., 2014). It is therefore recommended to conduct similar analyses on other urbanizing watersheds that have not yet experienced such a massive buildup, in order to evaluate urbanization impacts on hydrological regimes. Moreover, NOPs in other urbanizing watersheds should be examined for their effectiveness in environmental conservation.

5. Conclusions

This work addressed the future effects of urban development scenarios on rainfall-runoff relations for frequent rainfall events in an urbanized sub-basin, and possible land-use policy measures that could be implemented. The LC map analysis shows a linear trend of urbanization in the study area. Should this trend continue in the same direction and magnitude, by 2050, about 50% of the Ayalon sub-basin is expected to be covered by built-up areas. This trend corresponds to a gradual decrease in bare soil and orchard LCs, while forests and row crops, which are somewhat more protected by means of national regulations, are expected to undergo fewer changes. LCCs have corresponding effects on the runoff response. Future LC scenarios suggest a linear increase in the maximum discharge and runoff volume values as the urban landscape expands. These trends may be modified using within-city solutions such as BMPs (e.g. biofilters, infiltration trenches and porous pavement within public and private open spaces) and should be addressed by governmental and policy-making institutes and municipalities.

This LCC trend, however, is mostly apparent across the coastal plain. The hilly and mountainous parts, mostly governed by the Palestinian Authority, did not show projection simulations of a significant urban sprawl, but rather a higher urban density. This causes a dissonance between the two regions of this politically divided watershed. Change in policy and political status may lead to an accelerated urbanization in the PA region, which could multiply the effect of urban LC on runoff. To fully address this issue, both sides should agree on planning principles that will benefit the entire population of the Ayalon sub-basin.

Considering two authorized NOPs that account for open spaces within the watershed suggests that an afforestation trend along the hilly part of the sub-basin may have a moderate impact on the runoff response to frequent rainfall events. Mining and quarrying, if applied in the two determined locations, are not expected to change runoff flows, unless the runoff that reaches these quarries is collected and ponded.

The Yarkon-Ayalon sub-basin constitutes one of the most urbanized regions in Israel, and has undergone an intensive process of decentralization and urbanization in recent decades. This trend

is most likely to spread to adjacent watersheds, as population grows, transportation improves and demands for industrial, commercial and residential areas increase. As NOPs are not perfectly effective when attempting to manage and regulate urban development, national and statutory measures should be taken to address specific environmental features in order to contribute to a more sustainable hydrological regime.

Acknowledgements

This research was supported by the Kreitman School of Advanced Graduate Studies of Ben-Gurion University of the Negev, the Israel Water Authority, and the Ministry of Science and Technology via the Ramon Foundation, Israel. The authors would like to thank the Tel-Aviv District Planning and Building Commission for their cooperation and assistance and the Jacob Blaustein Institutes for Desert Research Remote Sensing Laboratory staff and students for their most appreciated support and knowledge sharing.

Disclosure statement

No potential conflict of interest was reported by the authors.

Funding

This work was supported by the The Ramon Foundation, The Israeli Ministry of Science and Technology [3-10673]; Israel Water Authority [4500686906].

References

AbuSada, J., & Thawaba, S. (2011). Multi cirteria analysis for locating sustainable suburban centers: A case study from ramallah governorate, palestine. *Cities*, *28*(5), 381–393. doi:10.1016/j.cities.2011.05.001

Alfasi, N., Almagor, J., & Benenson, I. (2012). The actual impact of comprehensive land-use plans: Insights from high resolution observations. *Land Use Policy*, *29*, 862–877. doi:10.1016/j.landusepol.2012.01.003

Alley, R.B., Marotzke, J., Nordhaus, W.D., Overpeck, J.T., Peteet, D.M., Jr., Pielke, R.A., … Wallace, J.M. (2003). Abrupt climate change. *Science*, *299*, 2005–2010. doi:10.1126/science.1081056

Antrop, M. (2004). Landscape change and the urbanization process in Europe. *Landscape and Urban Planning*, *67*, 9–26. doi:10.1016/S0169-2046(03)00026-4

Arbia, G., Benedetti, R., & Espa, G. (1999). Contextual classification in image analysis: An assessment of accuracy of ICM. *Computational Statistics & Data Analysis*, *30*(4), 443–455. doi:10.1016/S0167-9473(98)00104-2

Baltas, E.A., & Karaliolidou, M.C. (2008). Hydrological effects of land use and climate changes in northern Greece. *Journal of Land Use Science*, *2*(7), 225–241. doi:10.1080/17474230701622908

Bates, B., Kundzewicz, Z.W., Shaohong, W., & Palutikof, J. (2008). *Climate change and water. Technical paper on the intergovermental panel on climate change* (pp. 37, 48–49). Geneva: IPCC Secretariat.

Behan, K., Maoh, H., & Kanaroglou, P. (2008). Smart growth strategies, transportation and urban sprawl: Simulated futures for Hamilton, Ontario. *The Canadian Geographer*, *52*(3), 291–308. doi:10.1111/j.1541-0064.2008.00214.x

Black, R., Kniveton, D., Skeldon, R., Coppard, D., Murata, A., & Schmidt-Verkerk, K. (2008). *Demographics and climate change: Future trends and their policy implications for migration*. Brighton: Development Research Centre on Migration, Globalisation and Poverty. Brighton.

Brabec, E., Schulte, S., & Richards, P.L. (2002). Impervious surfaces and water quality: A review of current literature and its implications for watershed planning. *Journal of Planning Literature*, *16*(4), 499–514. doi:10.1177/088541202400903563

Bramley, G., & Kirk, K. (2005). Does planning make a difference to urban form? Recent evidence from Central Scotland. *Environment and Planning*, *37*, 355–378. doi:10.1068/a3619

Buitelaar, E., Galle, M., & Sorel, N. (2011). Plan-led planning sysems in development-led practices: An empirical analysis into the (lack of) institutionalisation of planning law. *Environment and Planning*, *43*, 928–941. doi:10.1068/a43400

Camacho Olmedo, M.T., Paegelow, M., & Mas, J.F. (2013). Interest in intermediate soft-classified maps in land change model validation: Suitability versus transition potential. *International Journal of Geographical Information Science*, *27*(12), 2343–2361. doi:10.1080/13658816.2013.831867

Carmon, N., Shamir, U., & Meiron-Pistiner, S. (1997). Water-sensitive urban planning: protecting groundwater. *Journal of Environmental Planning and Management*, *40*(4), 413–434. doi:10.1080/09640569712010

Chen, Y., Youpeng, X., & Yin, Y. (2009). Impacts of land use change scenarios on storm-runoff generation in Xitiaoxi basin, China. *Quaternary International*, *208*(1), 121–128. doi:10.1016/j.quaint.2008.12.014

Choi, B.-Y., Yun, S.-T., Soon-Young, Y., Lee, P.-K., Park, S.-S., Chae, G.-T., & Mayer, B. (2005). Hydrochemistry of urban groundwater in Seoul, South Korea: Effects of land-use and pollutant recharge. *Environmental Geology*, *48*(8), 979–990. doi:10.1007/s00254-004-1205-y

Choi, W., & Deal, B.M. (2008). Assessing hydrological impact of potential land use change through hydrological and land use change modeling for the Kishwaukee River basin (USA). *Journal of Environmental Management*, *88*(4), 1119–1130. doi:10.1016/j.jenvman.2007.06.001

County-of-Santa-Cruz-Planning-Department. (2009). Bonny Doon limestone quarry boundary expansion project and reclamation plan amendment final environmental impact report.

Darwish, T., Khater, C., Jomaa, I., Stehouwer, R., Shaban, A., & Hamzé, M. (2011). Environmental impact of quarries on natural resources in Lebanon. *Land Degradation & Development*, *22*, 345–358. doi:10.1002/ldr.1011

Deng, Z., Zhang, X., Li, D., & Pan, G. (2015). Simulation of land use/land cover change and its effects on the hydrological characteristics of the upper reaches of the Hanjiang Basin. *Environmental Earth Sciences*, *73*(3), 1119–1132. doi:10.1007/s12665-014-3465-5

Drescher, S.R., Law, N.L., Caraco, D.S., Cappiella, K.M., Schneider, J.A., & Hirschman, D.J. (2011). Research and policy implications for watershed management in the Atlantic Coastal Plain. *Journal of Coastal Management*, *39*(3), 242–258. doi:10.1080/08920753.2011.566123

Dwarakish, G.S., Ganasri, B.P., & De Stefano, L. (2015). Impact of land use change on hydrological systems: A review of current modeling approaches. *Cogent Geoscience*, *1*(1), 1115691. doi:10.1080/23312041.2015.1115691

Foody, G.M. (2004). Thematic map comparison: Evaluating the STATISTICAL SIGNIfiCANCE OF DIFFERENCES IN CLASSIfiCATION ACCURACY. *Photogrammetric Engineering & Remote Sensing*, *70*(5), 627–633. doi:10.14358/PERS.70.5.627

Fragkias, M., & Seto, K.C. (2012). The rise and rise of urban expansion. *Global Change*, *78*, 16–19.

Fredj, E., Silver, M., & Givati, A. (2015). An integrated simulation and distribution system for early flood warning. *International Journal of Computer and Information Technology*, *4*, 3.

Givati, A., Gochis, D.J., Rummler, T., & Kunstmann, H. (2016). Comparing one-way and two-way coupled hydrometeorological forecasting systems for flood forecasting in the Mediterranean region. *Hydrology*, *3*(2), 19. doi:10.3390/hydrology3020019

Gochis, D.J., Wei, Y., & Yates, D. (2015). *The WRF-Hydro model technical description and user's guide, version 3.0 NCAR Technical document*, Retrieved from: http://www.ral.ucar.edu/projects/wrf_hydro/.

Guan, M., Sillanpaa, N., & Koivusalo, H. (2016). Storm runoff response to rainfall pattern, magnitude and urbanization in a developing urban catchment. *Hydrological Processes*, *30*, 543–557. doi:10.1002/hyp.10624

Gvirtzman, H. (2002). *israel water resources, chapters in hydrology and environmental sciences*. Jerusalem: Yad Ben-Zvi Press.

Hamdi, R., Termonia, P., & Baguis, P. (2010). Effects of urbanization and climate change on surface runoff of the Brussels Capital Region: A case study using an urban soil-vegetation-atmosphere-transfer model. *International Journal of Climatology*. doi:10.1002/joc.2207

He, Y., Lin, K., & Chen, X. (2013). Effect of Land Use and Climate Change on Runoff in the Dongjiang Basin of South China. *Mathematical Problems in Engineering*, *2013*, 1–14. Article ID 471429. 10.1155/2013/471429

He, C. (2003). Integration of geographic information systems and simulation model for watershed management. *Environmental Modelling & Software*, *18*, 809–813. doi:10.1016/S1364-8152(03)00080-X

Hernandez, M., Miller, S.N., Goodrich, D.C., Goff, B.F., Kepner, W.G., Edmonds, C.M., & Jones, K.B. (2000). Modeling runoff response to land cover and rainfall spatial variability in semi-arid watersheds. *Environmental Monitoring and Assessment*, *64*(1), 285–298. doi:10.1023/A:1006445811859

Hirabayashi, Y., Mahendran, R., Koirala, S., Konoshima, L., Yamazaki, D., Watanabe, S., … Kanae, S. (2013). Global flood risk under climate change. *Nature Climate Change*, *3*(9), 816–821. doi:10.1038/nclimate1911

Hong, B., Limburg, K.E., Hall, M.H., Mountrakis, G., Groffman, P.M., Hyde, K., … Myers, S.J. (2012). An integrated monitoring/modeling framework for assessing human-nature interactions in urbanizing watersheds: Wappinger and onondaga creek watersheds, New York, USA. *Environmental Modelling & Software*, *32*, 1–15. doi:10.1016/j.envsoft.2011.08.006

Iovanna, R., & Vance, C. (2007). Modeling of continuous-time land cover change using satellite imagery: An application from North Carolina. *Journal of Land Use Science*, *2*(3), 147–166. doi:10.1080/17474230701623013

Irons, J.R., Markham, B.L., Nelson, R.F., Toll, D.L., Williams, D.L., Latty, R.S., & Stauffer, M.L. (1985). The effects of spatial resolution on the classification of Thematic Mapper data. *International Journal of Remote Sensing*, *6*(8), 1385–1403. doi:10.1080/01431168508948285

Israel, E., & Cohen-Blankshtain, G. (2010). Testing the decentralization effects of rail systems: Empirical findings from Israel. *Transportation Research Part A*, *44*, 523–536. doi:10.1016/j.tra.2010.03.021

Jacobson, C.R. (2011). Identification and quantification of the hydrological impacts of imperviousness in urban catchments: A review. *Journal of Environmental Management*, *92*, 1438–1448. doi:10.1016/j.jenvman.2011.01.018

Keppner, W.G., Ramsey, M.M., Brown, E.S., Jarchow, M.E., Dickinson, K.J.M., & Mark, A.F. (2012). Hydrologic futures: Using scenario analysis to evaluate impacts of forecasted land use Cchange on hydrologic services. *ESA Journals*, *3* (7), 1–25. doi:10.1890/ES11-00367.1

Khavich, V., & Ben-Zvi, A. (1995). Flash flood forecasting model for the Ayalon stream, Israel. *Hydrological Sciences Journal*, *40*(5), 599–613. doi:10.1080/02626669509491447

Kliot, N. (1986). Man's impact on river basins: An Israeli case study. *Applied Geography*, *6*(2), 163–178. doi:10.1016/0143-6228(86)90017-2

Kotter, T. (2004). *Risks and opportunities of urbanisation and megacities*. Paper presented at the Fig Working Week, 2004, Athens, Greece.

López, E., Bocco, G., Mendoza, M., & Duhau, E. (2001). Predicting land-cover and land-use change in the urban fringe A case in Morelia city, Mexico. *Landscape and Urban Planning*, *55*(4), 271–285. doi:10.1016/S0169-2046(01)00160-8

Lovinger, L., Nardy, G., & Malka, L. (2013). *Outline plan for drainage in Tel-Aviv-Yafo*.Tel-Aviv.

Mahmoud, S.H., Alazba, A.A., & Chapman, M.(.G. (2015). Hydrological response to land cover changes and human activities in arid regions using a geographic information system and remote sensing. *Plos One*, *10*(4), e0125805. doi:10.1371/journal.pone.0125805

Miller, J.D., Kim, H., Kjeldsen, T.R., Packman, J., Grebby, S., & Dearden, R. (2014). Assessing the impact of urbanization on storm runoff in a peri-urban catchment using historical change in impervious cover. *Journal of Hydrology*, *515*, 59–70. doi:10.1016/j.jhydrol.2014.04.011

Miralles, R., García-Sánchez, E., & Jordán, M.M. (2006). Hydrologic and geoenvironmental characterization of wetlands in quarries of the Vinalopó Mitjà (Alicante, Spain). *Environmental Geology*, *50*(7), 1053–1059. doi:10.1007/s00254-006-0277-2

Mishra, V.N., Rai, P.K., & Mohan, K. (2014). Prediction of land use changes based on land change modeler (LCM) using remote sensing: A case study of Muzaffarpur (Bihar), India. *Zbornik Radova Geografskog Instituta Jovan Cvijic, Sanu*, *64*(1), 111–127. doi:10.2298/IJGI1401111M

Moody, A., & Woodcock, C.E. (1995). The influence of scale and the spatial characteristics of landscapes on land-cover mapping using remote sensing. *Landscape Ecology*, *10*(6), 363–379. doi:10.1007/bf00130213

Munoz-Villers, L.E., & McDonnell, J.J. (2013). Land use change effects on runoff generation in a humid tropical montane cloud forest region. *Hydrology and Earth System Sciences*, *17*, 3543–3560. doi:10.5194/hess-17-3543-2013

Nash, J.E., & Sutcliffe, J.V. (1970). River flow forecasting through conceptual models part I — A discussion of principles. *Journal of Hydrology*, *10*(3), 282–290. doi:10.1016/0022-1694(70)90255-6

Neumann, B., Vafeidis, A.T., Zimmermann, J., & Nicholls, R.J. (2015). Future coastal population growth and exposure to sea-level rise and coastal flooding - a global assessment. *Plos One*, *10*(3), e0118571. doi:10.1371/journal.pone.0118571

Nirupama, N., & Simonovic, S.P. (2007). Increase of flood risk due to urbanisation: A Canadian example. *Natural Hazards*, *40*, 25–41. doi:10.1007/s11069-006-0003-0

Ohana-Levi, N., Karnieli, A., Egozi, R., Givati, A., & Peeters, A. (2015). Modelling the effects of land-cover change on rainfall-runoff relationships in a semi-arid, Eastern Mediterranean watershed. *Advances in Meteorology*, *2015*, 16. doi:10.1155/2015/838070

Ongsomwang, S., & Pimjai, M. (2015). Land use and land cover prediction and its impact on surface runoff. *Suranaree Journal of Science & Technology*, *22*(2), 205–223.

Orenstein, D.E., Bradley, B.A., Albert, J., Mustard, J.F., & Hamburg, S.P. (2011). How much is built? Quantifying and interpreting patterns of built space from different data sources. *International Journal of Remote Sensing*, *32*(9), 2621–2644. doi:10.1080/01431161003713036

Orenstein, D.E., & Hamburg, S.P. (2009). To populate or preserve? Evolving political-demographic and environmental paradigms in Israeli land-use policy. *Land Use Policy*, *26*, 984–1000. doi:10.1016/j.landusepol.2008.12.003

Paegelow, M., Olmedo, M.T.C, & Camacho. (2008). *Advances in geomatic simulations for environmental dynamics*. Verlag, Berlin, Hidelberg: Springer.pp.3-54.

Pauchard, A., Aguayo, M., Pena, E., & Urrutia, R. (2006). Multiple effects of urbanization on the biodiversity of developing countries: The case of a fast-growing metropolitan area (Concepcion, Chile). *Biological Covservation*, *127*, 272–281. doi:10.1016/j.biocon.2005.05.015

Pérez-Vega, A., Mas, J.-F., & Ligmann-Zielinska, A. (2012). Comparing two approaches to land use/cover change modeling and their implications for the assessment of biodiversity loss in a deciduous tropical forest. *Environmental Modelling & Software*, *29*(1), 11–23. doi:10.1016/j.envsoft.2011.09.011

Rahamimoff, A. (2005). *Master plan for the yarqon River - Summary of the Master Plan*. Ramat Gan, Israel.

Ronald, E.J. (2006). *IDRISI Andes Tutorial*. Worcester, MA: Clark Labs, Clark University.

Rulli, M.C., & Rosso, R. (2007). Hydrologic response of unpland catchments to wildfires. *Advances in Water Resources*, *30*, 2072–2086. doi:10.1016/j.advwatres.2006.10.012

Santillan, J., Makinano, M., & Paringit, E. (2011). Integrated Landsat image analysis and hydrologic modeling to detect impacts of 25-year land-cover change on surface runoff in a Philippine watershed. *Remote Sensing*, *3*(6), 1067–1087. doi:10.3390/rs3061067

Seto, K.C., Fragkias, M., Guneralp, B., & Reilly, M.K. (2011). A meta analysis of global urban land expansion. *Plos One*, *6* (8), e23777. doi:10.1371/journal.pone.0023777

Shachar, A. (1998). Reshaping the Map of Israel: A new national planning doctrine. *Annals of the American Academy of Political and Social Science*, *555*(1), 209–218. doi:10.1177/0002716298555001014

Shamir, U., & Carmon, N. 2007. Water sensitive planning : Integrating water considerations into Urban and Regional Planning. *Water and Environment Journal*, 24(3), 181–191.

Shields, C., & Tague, C. (2015). Ecohydrology in semiarid urban ecosystems: Modeling the relationship between connected impervious area and ecosystem productivity. *Water Resources Research*, *51*, 302–319. doi:10.1002/2014WR016108

Shoshany, M., & Goldshleger, N. (2002). Land-use and population density changes in Israel - 1950 to 1990: Analysis of regional and local ternds. *Land Use Policy*, *19*(2), 123–133. doi:10.1016/S0264-8377(02)00008-X

Sisay, E., Halefom, A., Khare, D., Singh, L., & Worku, T. (2017). Hydrological modelling of ungauged urban watershed using SWAT model. *Modeling Earth Systems and Environment*, *3*(2), 693–702. doi:10.1007/s40808-017-0328-6

Sonwalkar, M., Fang, L., & Sun, D. (2010). Use of NDVI dataset for a GIS based analysis: A sample study of TAR Creek superfund site. *Ecological Informatics*, *5*(6), 484–491. doi:10.1016/j.ecoinf.2010.07.003

Tal, D. (2015). *State of the Sea Report 2015*

Tian, L., & Shen, T. (2011). Evaluation of plan implementation in the transitional China: A case of Guangzhou city master plan. *Cities*, *28*, 11–27. doi:10.1016/j.cities.2010.07.002

Trimble, S.W. (1997). Contribution of Stream Channel Erosion to Sediment Yield from an Urbanizing Watershed. *Science*, *278*(5342), 1442–1444. doi:10.1126/science.278.5342.1442

UN. (2014). *World Urbanization Prospects: The 2014 Revision, Highlights*. Author.United Nations.

Weisthal, M. (2014). *Assessment of potential energy savings in Israel through climate-aware residential building design. (Master of Science)*. Ben-Gurion University of the Negev, Sede Boqer. Ben-Gurion University of the Negev.

York, A., Tuccillo, J., Boone, C., Bolin, B.O.B., Gentile, L., Schoon, B., & Kane, K. (2014). Zoning and land use: A tale of incompatibility and environmental injustice in early phoenix. *Journal of Urban Affairs*, *36*(5), 833–853. doi:10.1111/juaf.12076

Yu, P., Wang, Y., Coles, N., Xiong, W., & Xu, L. (2015). Simulation of runoff changes caused by cropland to forest coversion in the upper Yangtze River Region, SW China. *Plos One*, *10*(7), e0132395. doi:10.1371/journal.pone.0132395

Zahmatkesh, Z., Karamouz, M., Goharian, E., & Burian, S.J. (2014). Analysis of the effects of climate change on urban storm water runoff using statistically downscaled precipitation data and a change factor approach. *Journal of Hydrologic Engineering*, *20*(7), 05014022. doi:10.1061/(ASCE)HE.1943-5584.0001064

Zhang, Y., & Shuster, W. (2014). Impacts of spatial distribution of impervious areas on runoff response of hillslope catchments: Simulation study. *Journal of Hydrologic Engineering*, *19*(6), 1089–1100. doi:10.1061/(ASCE)HE.1943-5584.0000905